05| Оригинални научни рад
Research paper
doi 10.7251/STP1813096M ISSN 2566-4484

ULTIMATE STRENGTH OF COMPRESSED SLABS AND BOX GIRDERS

Dragan Milašinović, *ddmil@gf.uns.ac.rs*,
University of Novi Sad, Faculty of Civil Engineering, Subotica
Dijana Majstorović, *dijana.majstorovic@aggf.unibl.org*,
University of Banja Luka, Faculty of Architecture, Civil Engineering and Geodesy
Radovan Vukomanović, *radovan.vukomanovic@aggf.unibl.org*,
University of Banja Luka, Faculty of Architecture, Civil Engineering and Geodesy
Radomir Cvijić, *radomir.cvijic@aggf.unibl.org*,
University of Banja Luka, Faculty of Architecture, Civil Engineering and Geodesy

Abstract: A theoretical investigation into the effectiveness of a plate thickness against the ultimate strength of a compressed slabs and box girders is carried out. Series of the buckling analyses, the elastic, the viscoplastic and the ultimate strength are performed by the rheological-dynamical inelastic theory and the finite strip method on a slabs and box girders under thrust. In the analytical method, rheological-dynamical analogy (RDA) is introduced to express the critical stresses of slabs and box girders in the range of viscoplastic strains and strain hardening. Applying the finite strip method (FSM) as a semi-analytical method, the fundamental equilibrium equations are derived based on the principle of minimum total potential energy. Apart from the quantitative research the qualitative research is presented to demonstrate the capabilities of the present theory.

Keywords: slabs; box girders; elastic buckling; viscoplastic buckling; ultimate strength; FSM; RDA.

ГРАНИЧНА НОСИВОСТ ПРИТИСНУТИХ ПЛОЧА И САНДУЧАСТИХ НОСАЧА

Резиме: Извршено је теоријско истраживање утицаја промјене дебљине код притиснутих плоча и сандучастих носача на граничну носивост. Низ анализа извијања је спроведен. Реолошко-динамичком аналогијом и методом коначних трака одређена је еластична, вископластична и гранична носивост на притиснутим плочама и сандучастим носачима. Реолошко-динамичка аналогија (РДА) је кориштена у аналитичким изразима за добијање критичних напона анализираних носача у области вископластичних деформација и ојачања материјала. Употребом методом коначних трака (МКТ) као полуаналитичког метода изведене су једначине равнотеже на основу принципа минимума укупне потенцијалне енергије. Поред квантитативне анализе дат је и квалитативан приказ са циљем да се истакну могућности дате теорије.

Кључне ријечи: плоче; сандучасти носачи; еластично извијање; вископластично извијање; гранична носивост; МКТ; РДА

1. INTRODUCTION

In general, many structures are constructed by using slabs to reduce their weight and costs, and box girders to improve their rigidity and strength. The buckling strength of slabs and box girders increases with the increase of a plate thickness, but reaches its maximum limiting value when the ultimate strength reached. However, the investigation of the stability of structural elements under compressive loading incorporating in the analysis the inelastic material behavior is undoubtedly a complex subject [1-3].

The thin-walled structures are structures which are generally made by joining flat plates at their edges. An important sub-set of these structures, which are the main concern of this paper are essentially prismatic forms, such as slabs and box girders. The analysis of the behavior of these structures is done using the semi-analytical FSM. The FSM is based on the basis functions (or eigenfunctions), which are derived from the solution of the beam differential equation of transverse vibration, and proved to be an efficient tool for analysis a great deal of structures for which both geometry and material properties can be considered as constant along a main direction. This method was pioneered by Cheung [4], who combined the plane elasticity and the Kirchhoff plate theory. Wang and Dawe [5] have applied the elastic geometrically non-linear FSM to the large deflection and post-overall-buckling analysis of diaphragm-supported plate structures. The geometrically non-linear harmonic coupled finite strip method (HCFSM) is also one of the many procedures that can be applied to analyze the large-deflection and post-buckling behavior of slabs and box girders [6].

If uniformly compressed thin-walled structures undergo inelastic deformations, these structures generally sustain two sources of non-linearity (geometrical non-linearity due to large deflection and material non-linearity due to inelastic behavior). Due to the slender nature of the cross-sections, their behavior is inevitably complex, with several parallel buckling phenomena influencing performance and limit states. The analysis presented in this paper is based on the RDA [7, 8]. The RDA is a type of inelastic analysis, which transforms one category of very complicated material non-linear problems to simpler linear dynamic problems by using modal analysis [9]. In this paper, we present a new approach in which the ultimate strengths of slabs and box girders are investigated by RDA. For the analysis of these structures using FSM, an inelastic isotropic 2D constitutive matrix is derived in [10].

2. METHODS OF THEORETICAL ANALYSES

It is well known that an initially flat slab undergoes a primary buckling from an initially flat equilibrium state under external loads, if the loads are applied non-eccentrically. When the load is eccentrically applied, lateral deflection increases from the beginning of the loading, but the increase in deflection is small until the load is near to the buckling load. Furthermore, the interaction of two types of column buckling (failure) in box girders, local and global (Euler) column buckling, may generate an unstable coupled mode, rendering the structure highly sensitive to imperfections. To analyze such behavior, the geometrical non-linearity must be taken into account.

For a further increase of the load, plastification gradually takes place, and structure (flat slab or box girder) reaches its ultimate strength. For the analysis of this stage, the material non-linearity as well as the geometrical non-linearity must be taken into account.

2.1. BUCKLING ANALYSIS BY FSM

The non-linear strain-displacement relations in FSM can be predicted by combination of plane elasticity and the Kirchhoff plate theory. This has been accomplished in [6], by using the second-order terms of Green-Lagrange strains. However, since longitudinal loading is assumed here (see Fig. 1), the second-order terms are only necessary for the longitudinal normal strain

$$\varepsilon_y = \frac{\partial v_0}{\partial y} + \frac{1}{2}\left[\left(\frac{\partial u_0}{\partial y}\right)^2 + \left(\frac{\partial v_0}{\partial y}\right)^2 + \left(\frac{\partial w}{\partial y}\right)^2\right] - z\frac{\partial^2 w}{\partial y^2}, \tag{1}$$

where u_0 and v_0 are, respectively, displacements in the middle surface in x and y directions, and w is displacement in z direction.

In FSM, which combines elements of the classical Ritz method and the finite element method (FEM), the general form of the displacement function can be written as a product of polynomials and trigonometric functions [4]

$$f = \mathbf{Aq} = \sum_{m=1}^{r} Y_m(y) \sum_{k=1}^{c} \mathbf{N}_k(x)\mathbf{q}_{km}, \tag{2}$$

where $Y_m(y)$ are functions from the Ritz method, $N_k(x)$ are interpolation functions from FEM [4] and $\mathbf{q}_{km}$ is a vector representing the m-th term nodal displacements. r is an integer specifying the number of series terms chosen for approximation and c represents the number of nodal lines of a strip.

The most commonly used series are the basis functions (or eigenfunctions) which are derived from the solution of the beam vibration differential equation

$$\frac{\partial^4 Y}{\partial y^4} = \frac{\mu^4}{a^4} Y, \tag{3}$$

where a is the length of the strip and μ is a parameter.

The general form of the basis functions is

$$Y(y) = C_1 \sin\left(\frac{\mu \cdot y}{a}\right) + C_2 \cos\left(\frac{\mu \cdot y}{a}\right) + C_3 \sinh\left(\frac{\mu \cdot y}{a}\right) + C_4 \cosh\left(\frac{\mu \cdot y}{a}\right), \tag{4}$$

with the coefficients C_1, etc., to be determined by the boundary conditions. This has been worked out in the ref. [4] for various boundary conditions and is listed below for a simply supported strip only

$$Y_m(y) = \sin\left(\frac{\mu_m \cdot y}{a}\right), \quad (\mu_m = \pi, 2\pi, 3\pi, ...m \cdot \pi). \tag{5}$$

We define the local Degrees Of Freedom (DOFs) as the displacements u_0, v_0 and w, and the transverse slope amplitude $\varphi = \left(\frac{\partial w}{\partial x}\right)$ of a nodal line (DOFs=4), as shown in Fig. 1. The DOFs are also called generalized coordinates.

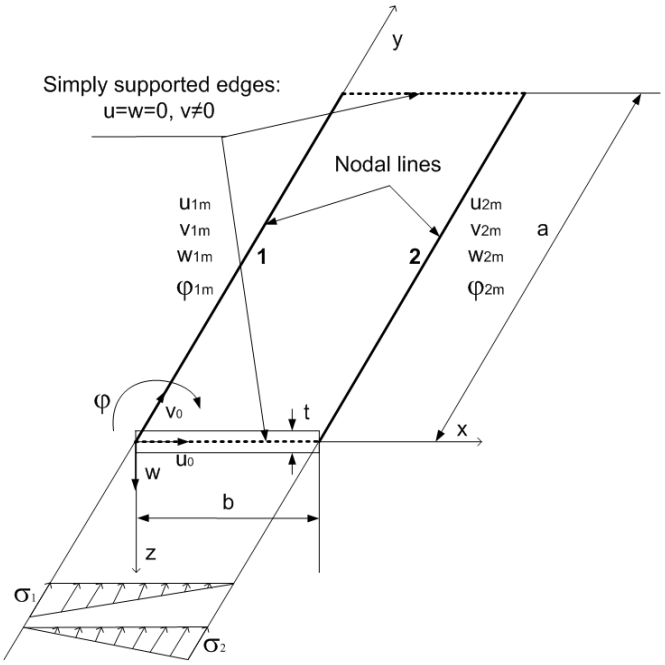

Figure 1. A simple supported strip with initial stresses.

The total potential energy of a strip is designated Π and is expressed with respect to the local DOFs [6]

$$\begin{aligned} \Pi &= U + W = \left(U_m + U_b\right) + W = \\ &= \left(1/2 \int_A \mathbf{q}_u^T \mathbf{B}_{u1}^T \mathbf{D}_m \mathbf{B}_{u1} \mathbf{q}_u \, dA + 1/2 \int_A \mathbf{q}_w^T \mathbf{B}_{w3}^T \mathbf{D}_b \mathbf{B}_{w3} \mathbf{q}_w \, dA \right) - \int_A \mathbf{q}^T \mathbf{A}^T \mathbf{p} dA. \end{aligned} \tag{6}$$

The conventional stiffness block matrices are, respectively [6]

$$\hat{\mathbf{K}}_{uu} = \int_A \mathbf{B}_{u1}^T \mathbf{D}_m \mathbf{B}_{u1} dA, \quad \hat{\mathbf{K}}_{ww} = \int_A \mathbf{B}_{w3}^T \mathbf{D}_b \mathbf{B}_{w3} dA, \tag{7}$$

where we introduce matrices, which are referred to as the strain matrices

$$\mathbf{B}_{u1} = \mathbf{L}_1 \mathbf{A}_u \, , \; \mathbf{B}_{w3} = \mathbf{L}_3 \mathbf{A}_w \, , \tag{8}$$

where

$$\mathbf{L}_1 = \begin{bmatrix} \partial/\partial x & 0 \\ 0 & \partial/\partial y \\ \partial/\partial y & \partial/\partial x \end{bmatrix}, \; \mathbf{L}_3 = \begin{bmatrix} -\partial^2/\partial x^2 \\ -\partial^2/\partial y^2 \\ -2 \cdot \partial^2/\partial x \partial y \end{bmatrix}, \tag{9}$$

and

$$\mathbf{A}_u = \begin{bmatrix} \mathbf{A}_u^u & \mathbf{0} \\ \mathbf{0} & \mathbf{A}_u^v \end{bmatrix}, \; \mathbf{q}_u = \begin{bmatrix} \mathbf{q}_u^u \\ \mathbf{q}_u^v \end{bmatrix}. \tag{10}$$

$\mathbf{A}_u^u$, $\mathbf{A}_u^v$ and $\mathbf{A}_w$ are the corresponding approximate functions, while $\mathbf{q}_u^u$, $\mathbf{q}_u^v$ and $\mathbf{q}_w$ represent vectors of displacement parameters in the nodal lines. The potential energy due to external surface loads **p** can be written simply as

$$W = -\int_A \mathbf{q}^T \mathbf{A}^T \mathbf{p} dA. \tag{11}$$

In order to obtain the equilibrium equations, the principle of minimum total potential energy is invoked

$$\frac{\partial \Pi}{\partial \mathbf{q}_m^T} = \mathbf{0}. \tag{12}$$

Eq. (12) gives a linear set of algebraic equations

$$\left(\hat{\mathbf{K}}_{uu}\mathbf{q}_u + \hat{\mathbf{K}}_{ww}\mathbf{q}_w\right) - \mathbf{Q} = \hat{\mathbf{K}}\mathbf{q} - \mathbf{Q} = \mathbf{0}, \tag{13}$$

where $\mathbf{Q}$ are the nodal forces.

Well known elements of the property matrices $\mathbf{D}_{\mathrm{m}}$ and $\mathbf{D}_{\mathrm{b}}$ for the orthotropic elastic material are

$$\begin{aligned} &K_x = \frac{E_x}{1-\mu_x\mu_y}, K_y = \frac{E_y}{1-\mu_x\mu_y}, K_1 = \frac{\mu_y E_x}{1-\mu_x\mu_y} = \frac{\mu_x E_y}{1-\mu_x\mu_y}, K_{xy} = G \\ &D_{m11} = K_x t, D_{m22} = K_y t, D_{m12} = K_1 t, D_{m66} = K_{xy} t \\ &D_{b11} = K_x \frac{t^3}{12}, D_{b22} = K_y \frac{t^3}{12}, D_{b12} = K_1 \frac{t^3}{12}, D_{b66} = K_{xy} \frac{t^3}{12}, \end{aligned} \tag{14}$$

where t is the thickness of a strip, Fig. 1.

Consider the simply supported flat strip shown in Fig. 1. The strip is subjected to an initial stress σ, which varies linearly from side 1 to side 2, but is constant along the longitudinal axis

$$\sigma_{ij} = \sigma_{22} = \sigma_y = \left(1 - \frac{x}{b}\right)\sigma_1 + \frac{x}{b}\sigma_2. \tag{15}$$

Considering the assigned stress distribution, from the non-linear strain tensor we include only the term given by Eq. (1). It is well known that the total potential energy of a strip is defined as the sum of its strain energy, potential energy due to nodal line forces, as well as the additional potential energy due to the initial stress.

As far as linear stability is concerned, the nodal forces $\mathbf{Q}$ are zero and it's therefore possible to derive the eigenvalue equation [6]

$$\left(\hat{\mathbf{K}} - \lambda \mathbf{K}_\sigma\right)\mathbf{q} = \mathbf{0}, \tag{16}$$

where $\hat{\mathbf{K}}$ is the conventional stiffness matrix, $\mathbf{K}_\sigma$ is the geometric stiffness matrix, λ is the eigenvalue (the load factor is compression positive), and $\mathbf{q}$ is the eigenvector (buckling mode). Based on Eq. (16) for one finite strip we can form the eigenvalue equations for a system of finite strips (mesh). The eigenvalue problem is to extract the solution pairs λ_{im} and $\mathbf{q}_{im}$ for all DOFs i, and all series terms m = 1,...,r. The buckling stresses are

$$\sigma_{im} = \frac{\lambda_{im}}{2 \cdot t}. \tag{17}$$

2.2. INELASTIC BUCKLING ANALYSIS BY FSM AND RDA

This section can be thought as an extension to Section 2.1. The purpose of developing a mathematical model for the rheological behavior of solids is to permit realistic results to be obtained from mathematical analyses of damaged structure under various conditions, such as micro cracking, which leads to its visco-plastic (VP) deforming and failure.

The FSM equilibrium equations (see Eq. 16) for a system exhibiting non-linear behavior can be written as

$$\left(\hat{\mathbf{K}}(\mathbf{C}) - \lambda \mathbf{K}_{\sigma}\right)\mathbf{q} = \mathbf{0}. \tag{18}$$

The non-linear term is the conventional stiffness matrix $\hat{\mathbf{K}}(\mathbf{C})$ of the system, which depends on the inelastic constitutive matrix **C**, according to the RDA. 2D compliance matrix $\mathbf{C}^{-1}$ is 'degenerated' directly from 3D theory [10] as follows

$$\begin{bmatrix} \varepsilon_x \\ \varepsilon_y \\ \gamma_{xy} \end{bmatrix} = \mathbf{C}^{-1} \begin{bmatrix} \sigma_x \\ \sigma_y \\ \tau_{xy} \end{bmatrix}, \quad \mathbf{C}^{-1} = \begin{bmatrix} 1/E_{Rx} & -e_{xy}/E_{Rx} & 0 \\ -e_{xy}/E_{Rx} & 1/E_{Ry} & 0 \\ 0 & 0 & 1/G_{Rxy} \end{bmatrix}, \tag{19}$$

where

$$\begin{aligned} &E_{Ry} = \frac{3E_H}{5-4\mu+2(1+\mu)\varphi_y}, E_{Rx} = \frac{3E_H}{5-4\mu+2(1+\mu)\varphi_x}, G_{Rxy} = \frac{G_H}{1+\sqrt{\varphi_x \varphi_y}}, \\ &e_{xy} = \frac{(7\mu-2)+(1+\mu)\varphi x}{5-4\mu+2(1+\mu)\varphi_x}, \varphi_x = \sigma_x K_E, \varphi_y = \sigma_y K_E. \end{aligned} \tag{20}$$

The RDA modulus iteration starts with the elastic constitutive matrix **D** (see $\mathbf{D}_{\mathrm{m}}$ and $\mathbf{D}_{\mathrm{b}}$)

$$\left(\hat{\mathbf{K}}(\mathbf{D}) - \lambda \mathbf{K}_{\sigma}\right)\mathbf{q} = \mathbf{0}. \tag{21}$$

This is a transcendental eigenvalue problem. Solving these equations, critical stresses $\sigma_{cry}^{(0)}$ can be obtained.

The corresponding VP slope is RDA modulus, which is the input parameter for the next iteration

$$E_{Ry}^{(1)} = \frac{3E_H}{5-4\mu+2(1+\mu)\sigma_{cry}^{(0)} \cdot K_E}, \tag{22}$$

where

$$K_E = \varphi \frac{3(1-\mu^2)}{\pi^2 E_H}\left(\frac{b}{t}\right)^2. \tag{23}$$

The first iteration gives the critical VP stress. The iterative procedure must be performed until there is convergence to the critical failure stress. The scheme of the modulus iterative method is illustrated in Fig. 2.

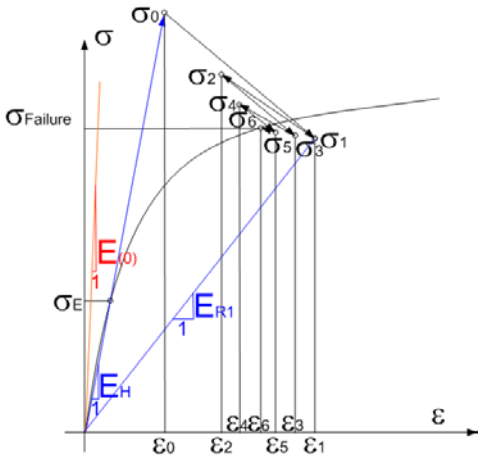

Figure 2. Scheme of the modulus iterative method.

3. NUMERICAL APPLICATIONS

Two examples are analyzed in this paper, compressed steel slab and box girder. The theoretical investigation into the effectiveness of the thickness against the ultimate strength is carried out. The transition from the various buckling modes by changing the lengths and thicknesses are examined and the elastic, VP and failure (ultimate strength) buckling curves are given.

3.1. SLABS

Consider the uniformly compressed rectangular steel slabs ($4.0 \geq a / b \geq 0.5$) depicted in Fig. 3, whose all edges are simply supported. Slabs of the following geometrical and elastic properties t = 16 mm, b = 1000 mm, E_H = 210 GPa and $\mu = 0.3$ were investigated using the FSM and RDA. The slab is divided into 6 finite strips with 7 nodal lines. Five series terms were included in the analysis.

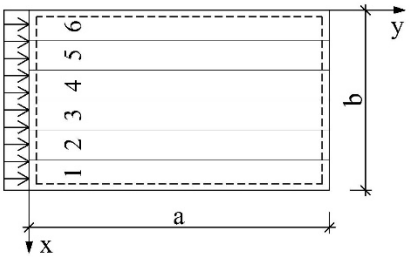

Figure 3. Uniformly compressed rectangular slab and finite strip idealization.

Fig. 4 shows the elastic buckling curve (critical stress versus a/b ratio). Critical stresses for three observed slab lengths of a = 1, 2 and 4 m are highlighted. As can be seen the same elastic critical stresses are obtained for different modes.

In order to obtain the inelastic quasi-static critical stresses, the Euler formula for buckling of an isolated plate strip was employed to find the structural-material constant K_E of plate, Eq. (23). The convergence of failure stress or ultimate strength for all a/b ratios is obtained using only six or seven iterations. The first iteration gives the VP yield stress.

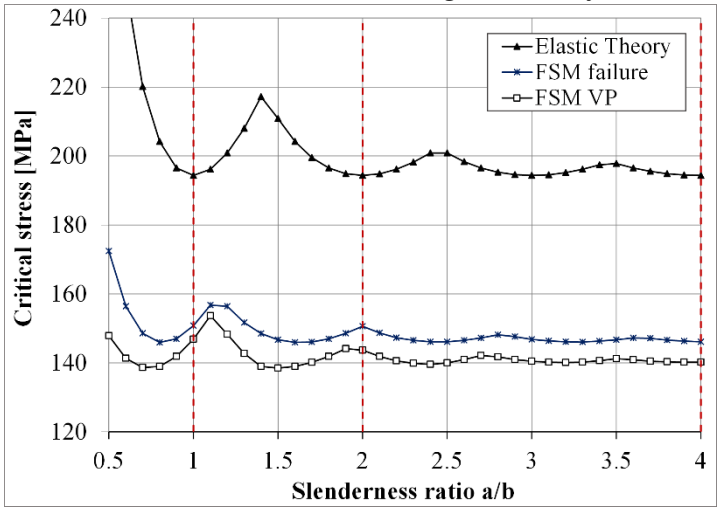

Figure 4. Elastic, VP and failure buckling curves for steel slab.

Inelastic critical stresses lag behind the elastic critical stresses across all modes, which is a consequence of the VP behavior of material that characterized by the delay time T^D [7]. As the length of slab is larger, the observed lag increases. Due to lag, the same slab length does not always correspond to the same mode at the elastic, VP and failure stresses. This phenomenon is named as mode interaction.

Fig. 5 shows critical stresses versus thickness for three observed slab lengths. It can be noticed that all stresses increase non-linear with increases of thickness.

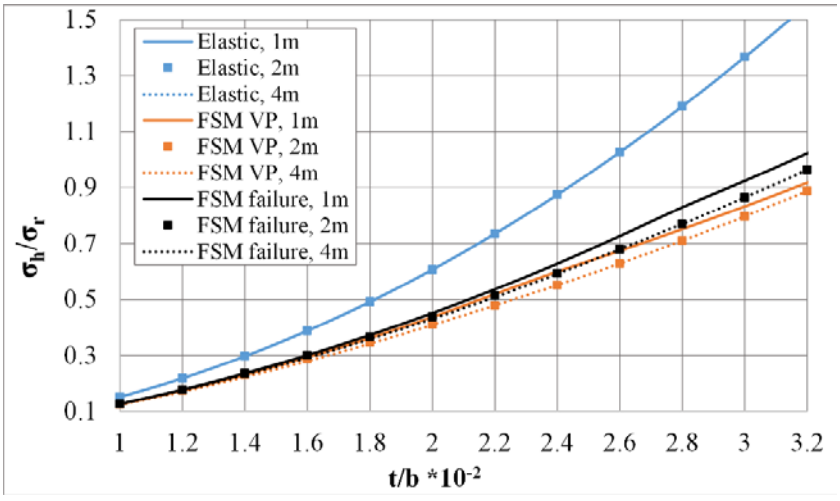

Figure 5. Critical stresses vs. thicknesses for three observed slab lengths.

Fig. 6 shows the load capacity or ultimate strength of slabs, as the 3D surface.

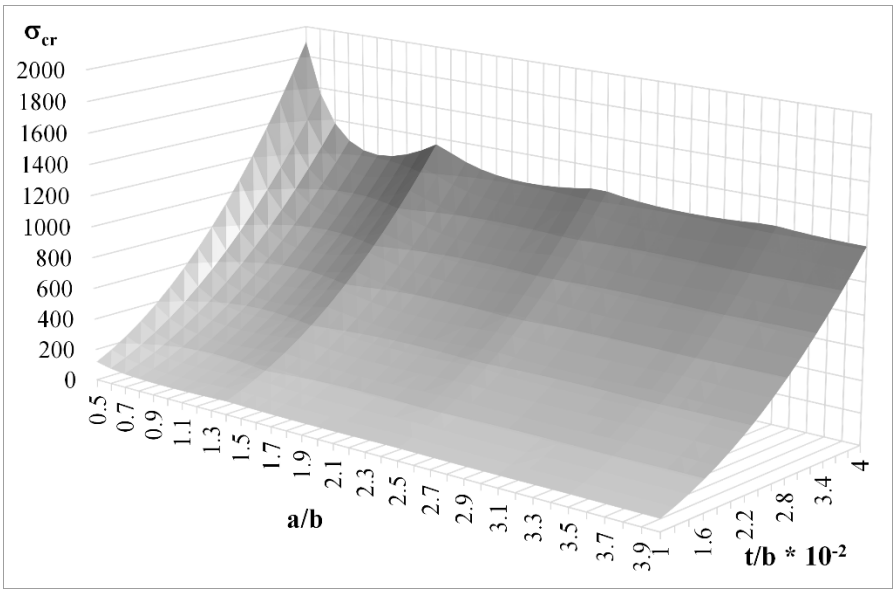

Figure 6. 3D surface of ultimate strength of slabs.

3.2. BOX GIRDERS

Simply supported ideally straight thin-walled box girder that consists of two webs of 100 mm and two flanges of 60 mm has been analyzed in details and results are compared with other theories for thickness of t = 2 mm [10, 11]. The girder is compressed axially. The elastic material properties are given in Fig. 7. In this paper the theoretical investigation into the effectiveness of the thickness against the ultimate strength is carried out.

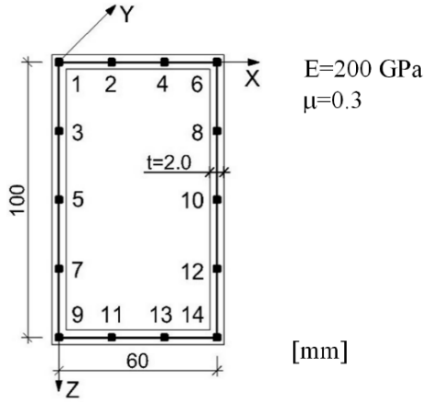

Figure 7. Thin-walled box girder and finite strip idealization.

The FSM elastic critical stresses computed with 14 finite strips and 8-35 series terms are shown in Fig. 8. Critical stresses for three observed girder lengths of a = 80, 120 and 400

mm are highlighted. Due to lag, the same girder length does not always correspond to the same mode at the elastic, VP and failure stresses. Consequently, the phenomenon of mode interaction is appeared again.

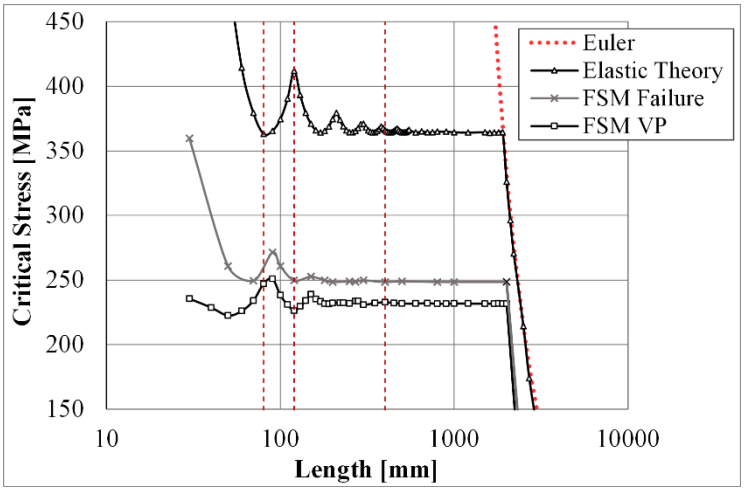

Figure 8. Elastic, visco-plastic and failure buckling curves for box girder.

Fig. 9 shows the change of stresses due to the change of thicknesses for three observed girder lengths. As can be seen, the non-linear changes of stresses are appeared up to a certain thickness, when the stresses stop to rise. This reduction of stresses is different for the elastic, VP and failure behavior of girders with strong dependents from the girder lengths.

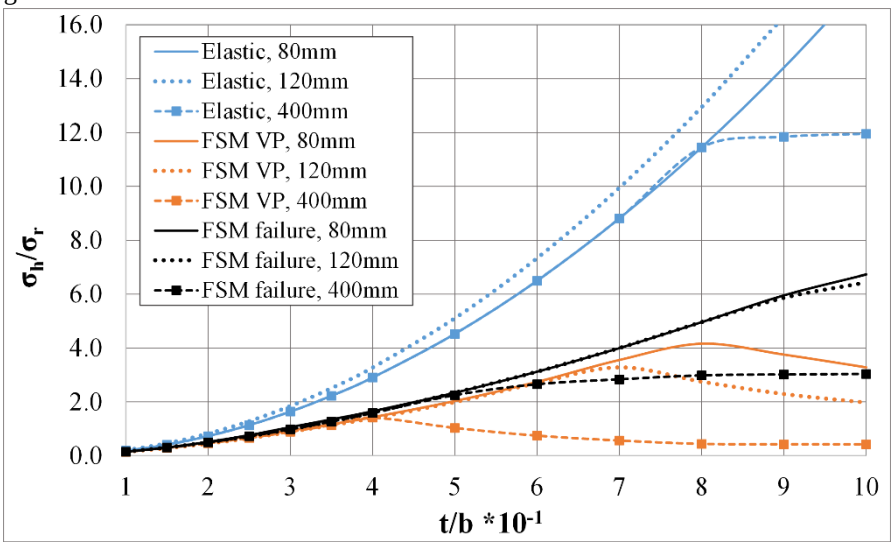

Figure 9. Critical stresses vs. thicknesses for three observed box girder lengths.

Results from the numerical studies for observed girder length of 400 mm that represent the influence of mode interactions on the buckling stresses are shown in Figs. 10 and 11.

Elastic interaction between local-global modes occurs in intermediate length of girders with near coincident critical stresses. The girders have the same lengths, but do not have all elastic characteristics in the same mode for small change of thickness. Because of that the girder loss of stability by local buckling for less thickness (t = 8 mm), while for higher thickness (t = 8.1 mm) the girder loss of stability by global buckling.

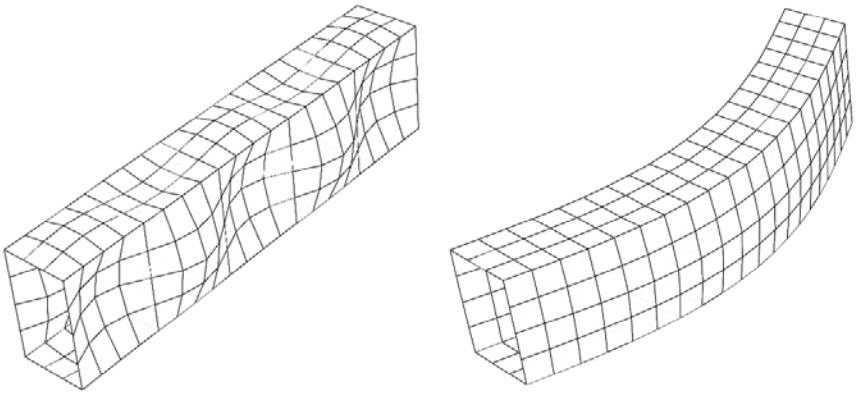

Figure 10. Buckling modes for length of 400 mm by FSM: local buckling (left - thickness of 8.0 mm) and global buckling (right - for thickness of 8.1 mm).

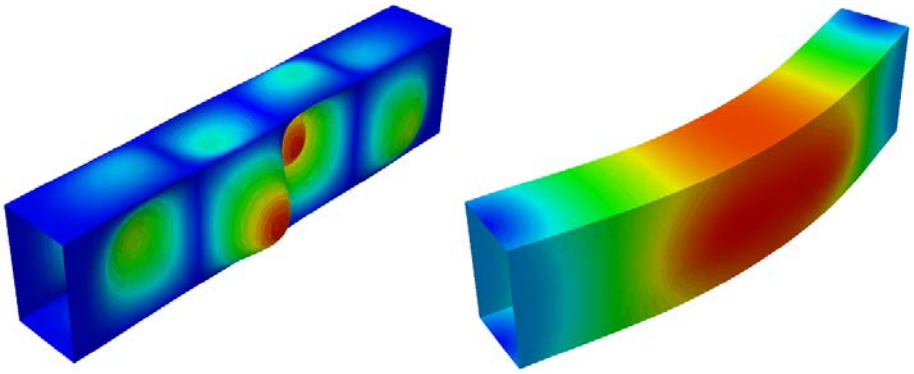

Figure 11. Buckling modes for length of 400 mm by Abaqus: local buckling (left - thickness of 8.6 mm) and global buckling (right - for thickness of 8.7 mm).

However, if we chose the thickness t = 2 mm, the above mentioned phenomena of elastic mode interaction appears on the girder length of 1900 mm in the global mode, Fig. 12, while the local mode defined the ultimate strength on the length of 1890 mm.

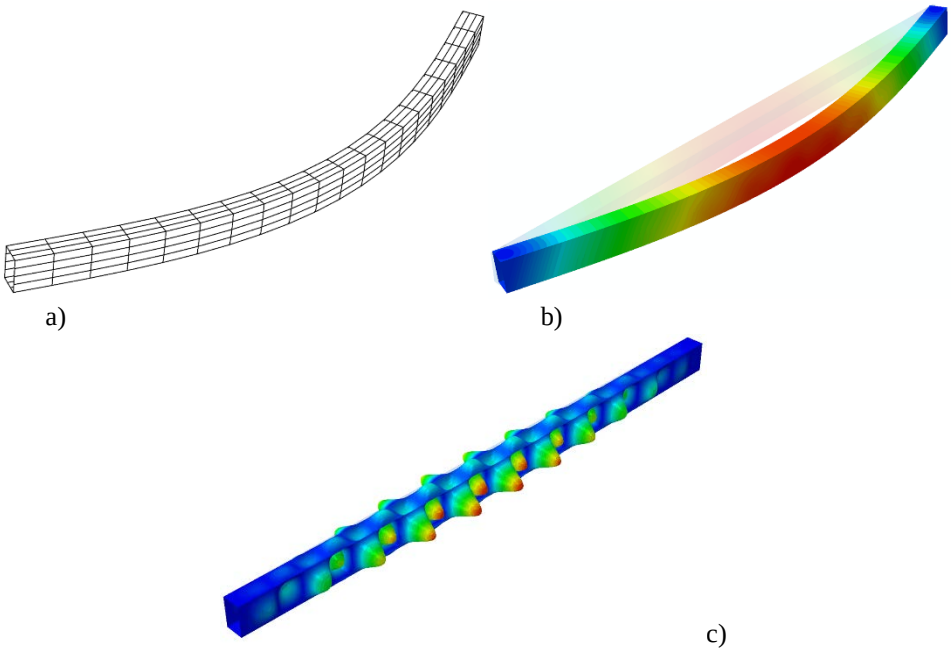

Figure 12. Global buckling modes for length of 1900mm: FSM (a), Abaqus (b) and local buckling mode for length of 1890mm with thickness of 2mm (c).

4. CONCLUSIONS

A theoretical investigation into the effectiveness of a plate thickness against the ultimate strength of a compressed slabs and box girders is carried out. The interaction between modes in the inelastic range of strains is analyzed taking into account the governing dynamic RDA modulus. The semi-analytical FSM eigenvalue analysis of slabs and box girders is used. The main indicators of capacity or collapse behavior are both the mode and the load (critical stress). Also the great influences on ultimate strength have both the length and thickness of slabs and box girders.

ACKNOWLEDGEMENTS

The work presented in this paper is a part of the investigation conducted within the research projects ON 174027 "Computational Mechanics in Structural Engineering" and TR 36017 "Utilization of by-products and recycled waste materials in concrete composites for sustainable construction development in Serbia: investigation and environmental assessment of possible applications", supported by the Ministry of Science and Technology of the Republic of Serbia. This support is gratefully acknowledged.

LITERATURE

[1] Ueda Y, Yao T. “Ultimate strength of compressed stiffened plates and minimum stiffness ratio of their stiffeners.” Engineering Structures, vol. 5, 1983, pp. 97–107.

[2] Suoza MA. “Coupled Dynamic Instability of Thin-Walled Structural Systems.” Thin-Walled Structures, vol. 20, 1994, pp. 139-149.

[3] Suoza MA, Bittencourt TN. “Viscoelastic Effects on the Vibration of Structural Elements Liable to Buckling.” Thin-Walled Structures, vol.12, 1991, pp. 281-239.

[4] Cheung YK. “Finite strip method in structural analysis.” Pergamon Press, 1976.

[5] Wang S, Dawe DJ. “Finite strip large deflection and post-overall-buckling analysis of diaphragm-supported plate structures.” Computers and Structures, vol. 61, no. 1, 1996, pp. 155-170.

[6] Milašinović DD. “The finite strip method in computational mechanics.” Faculties of Civil Engineering: University of Novi Sad, Technical University of Budapest and University of Belgrade: Subotica, Budapest, Belgrade, 1997.

[7] Milašinović DD. “Rheological-Dynamical analogy: modeling of fatigue behavior.” International Journal of Solids, vol. 40, no. 1, 2003, pp. 181–217.

[8] Milašinović DD. “Rheological-Dynamical analogy: prediction of damping parameters of hysteresis damper.” International Journal of Solids, vol. 44, no. 22-23, 2007, pp. 7143–7166.

[9] Milašinović DD. “Rheological-Dynamical analogy: design of viscoelastic and viscoplastic bar dampers.” Mechanics of Time-Dependent Materials, vol. 14, no. 4, 2010, pp. 389–409.

[10] Milašinović DD, Majstorović D, Vukomanović R. “Quasi static and dynamic inelastic buckling and failure of folded-plate structures by a full-energy finite strip method.” Advances in Engineering Software, vol. 117, 2018, pp. 136-152.

[11] Milašinović DD, Majstorović D, Vukomanović R, Mrđa N, Cvijić R. “Static and Dynamic Inelastic Buckling of Thin-Walled Structures Using The Finite Strip Method”. Proceedings of the International Scientific Conference on Planning, Design, Construct and Renewal in the Civil Engineering, iNDiS 2015, Faculty of Technical Sciences, Novi Sad, Serbia, 978-86-7892-750-8, 2015, pp. 67-73.